THE JOURNAL OF BIOLOGICAL CHEMISTRY VOL. 282, NO. 31, pp. 22747–22756, August 3, 2007

Characterization of the Properties and Trafficking of an Anchorless Form of the Prion Protein*[S]

Received for publication, February 20, 2007, and in revised form, June 6, 2007 Published, JBC Papers in Press, June 7, 2007, DOI 10.1074/jbc.M701468200

Vincenza Campana[‡], Anna Caputo[§], Daniela Sarnataro[§], Simona Paladino[‡¶], Simona Tivodar[§], and Chiara Zurzolo[‡§1]

From the [‡]Unité de Trafic Membranaire et Pathogénèse, Institut Pasteur, 25 rue du Docteur Roux, 75724 Paris Cedex 15, France and [§]Dipartimento di Biologia e Patologia Cellulare e Molecolare and [¶]Centro di Eccellenza di Ingegneria Genetica, Centro di Biotecnologie Avanzate, Università degli Studi di Napoli "Federico II," via Pansini 5, 80131 Napoli, Italy

Conversion of PrP^C into PrP^{Sc} is the central event in the pathogenesis of transmissible prion diseases. Although the molecular basis of this event and the intracellular compartment where it occurs are not yet understood, the association of PrP with cellular membranes and in particular its presence in detergent-resistant microdomains appears to be of critical importance. In addition it appears that scrapie conversion requires membrane-bound glycosylphosphatidylinositol (GPI)-linked PrP. The GPI anchor may affect either the conformation, the intracellular localization, or the association of the prion protein with specific membrane domains. However, how this occurs is not known. To understand the relevance of the GPI anchor for the cellular behavior of PrP, we have studied the biosynthesis and localization of a PrP version which lacks the GPI anchor attachment signal (PrPΔGPI). We found that PrPΔGPI is tethered to cell membranes and associates to membrane detergent-resistant microdomains but does not assume a transmembrane topology. Differently to PrP^C, this protein does not localize at the cell surface but is mainly released in the culture media in a fully glycosylated soluble form. The cellular behavior of anchorless PrP explains why PrPΔGPI Tg mice can be infected but do not show the classical signs of the disorder, thus indicating that the plasma membrane localization of PrP^C and/or of the converted scrapie form might be necessary for the development of a symptomatic disease.

According to the "protein only" hypothesis (1), the infectious agent of transmissible spongiform encephalopathies is an abnormally folded β-sheet-enriched conformer of the cellular prion protein (PrP^C),[2] called PrP scrapie (PrP^{Sc}) or prion (1). PrP^{Sc} is able to replicate and propagate itself by transferring its altered conformation to the endogenous PrP^C, a cell surface-enriched protein that becomes partially resistant to proteases and accumulates in plaques in the brain (2). The molecular basis of PrP^C-PrP^{Sc} conversion, the intracellular compartment where the conversion occurs, and how the process leads to neurological dysfunction are still very open and debated questions (3).

Several studies indicate that PrP^C-PrP^{Sc} conversion is a post-translational event that occurs after the protein reaches the cell surface (4–6). Indeed, it is possible to impair PrP^{Sc} formation in infected cells either by preventing PrP^C transport to the plasma membrane (7), by exposing PrP^C to specific antibodies, or by releasing it from the cell surface by different methods (4, 5) (for review, see Ref. 3). However, these data do not distinguish whether scrapie conversion occurs on the plasma membrane or later during its internalization. In infected cells PrP^{Sc} accumulates in late endosomes, and inhibition of endocytosis reduces scrapie production (5, 8), thus indicating that the endolysosomal pathway could be also involved in scrapie formation.

Although the exact nature of the compartment of prion conversion is still debated, the membrane domains (also called rafts) with which PrP associates seems to be important in the conversion process (3, 9–11). Rafts are membrane domains enriched in cholesterol and sphingolipids that have been proposed to have a central role in many cellular processes (12), including membrane sorting and trafficking, cell polarization, and signal transduction (13–15). Like other GPI-anchored proteins, PrP^C and PrP^{Sc} associate with rafts because of the affinity of their GPI anchor for saturated lipid species (16–19). In prion-infected N2a cells, perturbation of PrP raft association by modifying the cellular levels of cholesterol affects PrP^{Sc} formation (9–11). Moreover, removal of PrP^C from rafts by the substitution of its GPI anchor with a transmembrane domain prevents the formation of PrP^{Sc} (11, 20), thus suggesting a role for these microdomains in scrapie replication.

From these observations it also seems evident that scrapie conversion requires membrane-bound GPI-linked PrP. However, the role of the GPI-anchor in prion conversion is still debated. In cell-free experiments, PrP lacking the GPI moiety can be converted to the PrP^{Sc} form (21, 22), whereas in scrapie-

* This work was supported by grants from Ministero dell'Università e della Ricerca Scientifica e Tecnologica (FIRB 2003, PRIN 2006), the Telethon Foundation (GGP0414), European Union (FP6 LSHBCT 2006-019090), and Agence Nationale de la Recherche (NT-05-4 41767) (to C. Z.). The costs of publication of this article were defrayed in part by the payment of page charges. This article must therefore be hereby marked "*advertisement*" in accordance with 18 U.S.C. Section 1734 solely to indicate this fact.

[S] The on-line version of this article (available at http://www.jbc.org) contains supplemental Fig. 1.

[1] To whom correspondence should be addressed. Tel.: 33-01-45688277; Fax: 33-01-40613238; E-mail: zurzolo@pasteur.fr (Institut Pasteur) or Tel.: 39-081-7463237; Fax: 39-081-7701016; E-mail: zurzolo@unina.it (Università degli Studi di Napoli "Federico II").

[2] The abbreviations used are: PrP^C, cellular prion protein; PrP^{Sc}, scrapie prion protein; βCD, methyl-β-cyclodextrin; CNX, calnexin; DRM, detergent-resistant membrane domain; EndoH, endoglycosidase H; ER, endoplasmic reticulum; FRT, Fischer rat thyroid; GPI, glycosylphosphatidylinositol; PM, plasma membrane; PK, proteinase K; TX-100, Triton X-100; PGNaseF, peptide *N*-glycosidase F; PBS, phosphate-buffered saline; TRITC, tetramethylrhodamine isothiocyanate.

infected cells the absence of the GPI moiety reduces conversion (4, 23). Furthermore, it has been recently shown that a PrP mutant lacking the GPI anchor (anchorless PrP or PrPΔGPI) supports scrapie replication in transgenic mice, although the infected mice do not show any of the clinical signs of the disease until death (24). A possible explanation for these differences between PrP^{C} and PrPΔGPI could be that PrPΔGPI is *per se* able to sustain conversion into PrP^{Sc} but that other factors present in specific compartments of the cell are also required for conversion and for the pathogenesis of the disease. These findings have prompted us to analyze the biosynthesis, intracellular trafficking, and biological properties of an anchorless version of PrP (PrPΔGPI) in transfected cells to better understand the role of the GPI anchor in the behavior of the prion protein. Differently to what was published before, we found that PrPΔGPI is fully glycosylated, but in contrast to the GPI-anchored version, it does not localize on the plasma membrane and is mainly secreted. Interestingly, despite the lack of the GPI anchor, PrPΔGPI associates to intracellular membranes but does not acquire a transmembrane topology. Furthermore, we found that a significant amount of the protein associates to detergent-resistant domains (DRMs), supporting previous evidence that PrP^{C} could associate to lipid rafts in a GPI anchor-independent manner (25). We propose that the differences in metabolism and intracellular trafficking compared with PrP^{C} are relevant for the development of prion diseases and might lead to a better understanding of their pathogenic mechanisms.

EXPERIMENTAL PROCEDURES

Reagents and Antibodies—Cell culture reagents were purchased from Invitrogen. The α-PrP antibodies PRI308, SAF32, and SAF61 were a kind gift of Dr. J. Grassi (Commissariat à l'Energie Atomique, Saclay, France). The antibodies against α-calnexin (CNX) and early endosomal antigen 1 were from StressGen Biotechnologies Corp. (Victoria, BC, Canada). The antibody against Giantin was from Berkeley Antibody Co., Inc. (Richmond, CA). Lysotracker Red DND-99 was from Molecular Probes (Eugene, OR). Endoglycosidase H (EndoH) was from Roche Diagnostic, and peptide *N*-glycosidase F (PGNaseF) and neuraminidase were from Roche Applied Science. GM6001 (Ilomastat) matrix metalloprotease inhibitor was from Chemicon International. Protein-A-Sepharose was from GE Healthcare. Sulfo-H-hydroxy-biotin (S-NHS-biotin) was from Pierce. Methyl-β-cyclodextrin (βCD), mevinolin, fumonisin B1 and all other reagents were obtained from Sigma.

PrP Constructs and Transfection—Fischer rat thyroid (FRT) cells were transfected with a cDNA encoding 3F4-tagged PrPΔGPI (a kind gift of Dr. Sylvain Lehmann, UPR CNRS1142, Montpellier, France) with the calcium phosphate procedure as previously described (26), and single stable clones were selected by G418 resistance and used for the following experiments.

Cell Culture and Drug Treatments—FRT cells stably expressing PrPΔGPI were grown in F-12 Coon's modified medium containing 5% fetal bovine serum. Tunicamycin (10 μg/ml) was added to the cell culture medium for 16 h. Mevinolin/βCD and fumonisin B1 treatments were carried out as described elsewhere (16, 17). Cellular cholesterol levels before and after depletion were determined by a colorimetric assay (Infinity Cholesterol reagent; Sigma) according to the suggested Sigma protocol number 401, as previously described (17). The samples were then read in a spectrophotometer at 550 nm. Phorbol 12-myristate 13-acetate (1 μM), GM6001 (25 μM), and βCD (5 mM) were added to the culture medium for 7 h before collecting cell-free media.

Immunoprecipitation—Cells grown in 60- or 100-mm dishes were washed 3 times with and lysed in Triton/DOC buffer (0.5% Triton X-100, 0.5% DOC, 150 mM NaCl, 50 mM Tris-HCl, pH 7.5) with protease inhibitor mixture (leupeptin, antipain, pepstatin, and 1 mM phenylmethylsulfonyl fluoride) for 20 min. Lysates were then precleared with protein-A-Sepharose beads (5 mg/sample) for 30 min and incubated overnight at 4 °C with α-PrP antibody coupled with protein-A-Sepharose beads (10 mg/sample). For media analysis cell media were collected at 7 h or after overnight incubation and immunoprecipitated. The pellets were washed twice with cold lysis buffer and three times with PBS. The samples were then boiled with SDS sample buffer, loaded on polyacrylamide gels, and revealed by Western blotting against PrP and ECL. For direct coupling of antibody to protein A-Sepharose beads, 10 mg/sample of protein A-Sepharose beads was incubated with the antibody for 1 h at room temperature with gentle rocking. The beads were then washed and incubated in 20 mM methyl pimelimidate in 0.2 M sodium borate, pH 9.0, for 30 min at room temperature. The reaction was stopped with 0.2 M ethanolamine.

Peptide N-glycosidase F, Endoglycosidase H, and Neuraminidase Treatment—PGNaseF, EndoH, and neuraminidase digestions were performed on immunoprecipitated samples. For PGNaseF treatment the immunoprecipitated samples were resuspended and boiled for 5 min in 10 mM EDTA, 1% Triton X-100, 0.1% SDS, 1% β-mercaptoethanol and incubated with PGNaseF (5 units/sample) for 16 h at 37 °C.

For EndoH and neuraminidase (5 milliunits/sample) digestion, the immunoprecipitated samples were first boiled for 3 min in 50 μl of 0.1 M sodium citrate, pH 5.5, containing 0.1% SDS and then treated with the specific enzyme for 16 h at 37 °C. The samples were then analyzed by SDS-PAGE and Western blotting.

Pulse-Chase Analysis—FRT cells expressing PrPΔGPI and grown on 100-mm dishes were pulsed for 20 min with 100 μCi/ml [^{35}S]methionine and chased for various times at 37 °C, as indicated in Fig. 1*C*. At the end of the chase times cells were washed with cold PBS and lysed for 20 min on ice in Triton/DOC buffer. PrPΔGPI immunoprecipitation was performed overnight using the α-PrP SAF32 antibody coupled to protein-A-Sepharose beads. The pellets were washed twice with cold lysis buffer and three times with PBS. The samples were then boiled with SDS sample buffer, loaded on 12% polyacrylamide gels, and revealed by phosphorimaging scanning.

Assays for Scrapie-like Properties—Proteinase K (PK) digestion and Triton/DOC insolubility assays were performed as previously described (16, 27).

Fluorescence Microscopy—FRT cells stably expressing PrPΔGPI were grown for 4–5 days both on coverslips and on Transwell filters (not shown), washed with PBS, fixed in 2% paraformaldehyde, permeabilized with 0.075% saponin, and processed for indirect immunofluorescence using specific anti-

bodies. PrPΔGPI was visualized with a fluorescein isothiocyanate-conjugated secondary antibody, whereas CNX, giantin, and early endosomal antigen 1 were revealed by TRITC-conjugated secondary antibodies using a Zeiss laser scanning confocal microscope (LSCM 510). For lysosome staining, cells were incubated for 1 h with Lysotracker (1:10,000) in complete medium before fixing.

Biotinylation Assays—Confluent monolayers on Transwells were biotinylated and processed for immunoprecipitation as previously described (26). To recover the immunoprecipitated PrP, the samples were boiled for 10 min and then loaded on 12% gels and revealed by Western blotting with horseradish peroxidase-conjugated streptavidin.

Triton X-114 Phase Separation—Cells were lysed in Tris-buffered saline 1% Triton X-114 (10 mM Tris-HCl, pH 7.4, 150 mM NaCl. and 1 mM EDTA) for 1 h at 4 °C. Post-nuclear supernatants were incubated for 3 min at 37 °C and centrifuged for 1 min at room temperature for phase separation. An aqueous and a detergent phase were collected and trichloroacetic acid-precipitated. PrPs were revealed by Western blotting.

Topology Assays; Digitonin Permeabilization—FRT cells grown for 4–5 days on coverslips were washed twice with Buffer 1 (20 mM Hepes-KOH, pH 7.2, 110 mM potassium acetate, 2 mM magnesium acetate) and then incubated on ice for 5 min with digitonin (20 μg/ml) in Buffer 1. After washing, coverslips were fixed in 2% paraformaldehyde and, where indicated, permeabilized with 0.075% saponin, processed for indirect immunofluorescence, and analyzed by a Zeiss laser scanning confocal microscope (LSCM 510) as described above.

PK Protection Assay—Membrane topology of PrPΔGPI was determined as previously described (28, 29). Cells were lysed in 0.25 M sucrose, 10 mM HEPES, pH 7.4, by 10 passages through 26-gauge needles. The post-nuclear supernatant was divided into three samples; one untreated, the second digested with 250 μg/ml PK for 30 min at 22 °C in 50 mM Tris-HCl, pH 7.5, and the third digested with PK at the same concentration in the presence of 0.5% Triton X-100 (TX-100). Samples were immunoprecipitated both with SAF32 or SAF61 antibodies, divided in two aliquots digested (+) or not (−) with PGNaseF, and analyzed by Western blotting.

Sodium Carbonate Extraction—Cells were homogenized in 0.25 M sucrose with either 0.1 M Tris-HCl, pH 7.5, or 0.2 M sodium carbonate, pH 11, for 30 min on ice by 10 passages through 26-gauge needles and centrifuged for 30 min at 4 °C at 61,000 rpm (in a MLA 130 rotor from TLA 100, Beckman Instruments, Fullerton, CA). Soluble and insoluble phases were collected and trichloroacetic acid-precipitated, and PrPs were revealed by Western blotting.

DRM Analysis by Sucrose Density Gradients—Control and mevinolin/βCD- and fumonisin B1-treated cells grown to confluence in 150-mm dishes were harvested in cold PBS and resuspended in 1 ml of lysis buffer (1% TX-100, 10 mM Tris-HCl, pH 7.5, 150 mM NaCl, 5 mM EDTA), left in ice for 20 min, and passaged 10 times through 22-gauge needles. Lysates were mixed with an equal volume of 85% sucrose (w/v) in 10 mM Tris-HCl, pH 7.5, 150 mM NaCl, 5 mM EDTA, placed at the bottom of a discontinuous sucrose gradient (30–5%) in the same buffer, and ultracentrifuged at 200,000 × *g* for 17 h at 4 °C in an ultracentrifuge (SW41 rotor from Beckman Instruments). Twelve fractions were harvested from the top of the gradient. A white light-scattering band, identified in fraction 5 at the interface between 5 and 30% sucrose, contained DRM domains. Samples were trichloroacetic acid-precipitated, and proteins were analyzed by Western blotting.

Lipid Analysis—Aliquots of fraction 5 (800 μl) of sucrose density gradients diluted with 200 μl of lysis buffer were precleared twice with Dynabeads for 2 h and incubated overnight at 4 °C with an α-PrP antibody. Immunoprecipitates were recovered using protein A-coupled magnetic beads (30). ⅕ of the samples were analyzed by SDS-PAGE. Lipids were extracted from the immunoprecipitates and analyzed as described below. Cholesterol was quantified after separation on high performance TLC by visualization with 15% concentrated sulfuric acid in 1-butanol (30). Phospholipids and sphingomyelin were separated by a two-run mono-dimensional high performance TLC using the solvent system chloroform/methanol 9:1 (v/v) followed by the solvent system chloroform/methanol/acetic acid/water 30:20:2:1 (v/v/v/v) and quantified after separation on a high performance TLC followed by specific detection with a molybdate reagent. Lipids were quantified by densitometry and compared with known amounts of standard lipids (Molecular Analyst program, Bio-Rad).

Preparation of Detergent-free Lipid Rafts—Detergent-free extraction and gradients were performed as previously published (31). Four 150-mm plates of cells were washed and scraped into 20 mM Tris-HCl, pH 7.8, 250 mM sucrose to which had been added 1 mM $CaCl_2$ and 1 mM $MgCl_2$. Cells were pelleted by centrifugation for 2 min at 250 × *g* and resuspended in 1 ml of 20 mM Tris-HCl, pH 7.8, 250 mM sucrose containing 1 mM $CaCl_2$, 1 mM $MgCl_2$, and protease inhibitors at final concentrations of 0.2 mM aminoethylbenzenesulfonyl fluoride, 1 μg/ml aprotinin, 10 μM bestatin, 3 μM E-64, 10 μg/ml leupeptin, 2 μM pepstatin, and 50 μg/ml calpain inhibitor I. The cells were then lysed by passage through a 22-gauge needle 20 times. Lysates were centrifuged at 1000 × *g* for 10 min. The resulting post-nuclear supernatant was collected and transferred to a separate tube. The pellet was again lysed by the addition of 1 ml of base buffer plus divalent cations and protease inhibitors followed by sheering 20 times through a needle and syringe. After centrifugation at 1000 × *g* for 10 min, the second post-nuclear supernatant was combined with the first. An equal volume (2 ml) of 20 mM Tris-HCl, pH 7.8, 250 mM sucrose containing 50% OptiPrep was added to the combined post-nuclear supernatants and placed in the bottom of a 12-ml centrifuge tube. An 8-ml gradient of 0–20% OptiPrep in base buffer was poured on top of the lysate, which was now 25% in OptiPrep. Gradients were centrifuged for 90 min at 52,000 × *g* using an SW-41 rotor in a Beckman ultracentrifuge. Gradients were fractionated into 0.67-ml fractions, and the distribution of various proteins was assessed by Western blotting.

Differential Centrifugation and Secreted Vesicle Isolation—Cell culture media from 20 × 10^6 FRT cells was submitted to differential centrifugation in the absence or in the presence of 1% TX-100. Media were centrifuged at 1,000 × *g* for 5 min and at 10,000 × *g* for 30 min and ultracentrifuged at 100,000 × *g* for 1 h. Pellet and soluble fractions were recovered at each ultra-

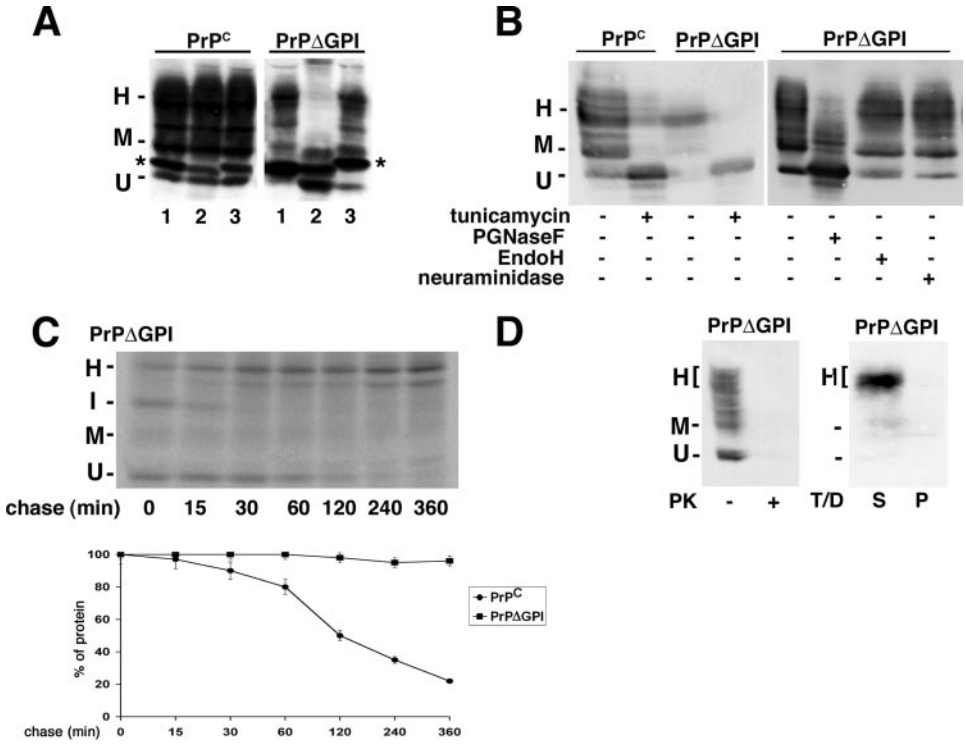

FIGURE 1. **PrPΔGPI is diglycosylated, has a long half-life, and does not acquire scrapie-like characteristics in transfected FRT cells.** *A*, FRT cells expressing PrP^C and PrPΔGPI were lysed in Triton/DOC, and PrP isoforms were immunoprecipitated by using either an α-N-terminal PrP (SAF32) (*lanes 1*), an α-3F4 tag (PRI308) (*lanes 2*), or an α-C-terminal PrP (SAF61) (*lanes 3*) antibody, and PrPs were analyzed by SDS-PAGE and Western blot by using SAF32 antibody. *B*, cells were grown in the presence (+) or absence (−) of tunicamycin for 16 h and then lysed in Triton/DOC buffer. The proteins were then trichloroacetic acid-precipitated, separated by SDS-PAGE, and immunoblotted against α-PrP antibody (*left panel*). In the *right panel*, PrPΔGPI was either untreated or digested for 16 h with PGNaseF, EndoH, or neuraminidase. After immunoprecipitation with SAF32, PrPΔGPI was revealed by SDS-PAGE and Western blotting. *C*, FRT cells expressing either PrP^C or PrPΔGPI were pulse-labeled with [^{35}S]methionine for 20 min and then chased in medium containing unlabeled methionine for the indicated times. Cells were then lysed in Triton/DOC buffer, and PrP was immunoprecipitated. Samples were analyzed by SDS-PAGE and phosphorimaging scanning. Quantization of three independent experiments is shown in the graphs. *Error bars* are given from the different quantization. *D*, PK digestion assay. After lysis in the absence of protease inhibitors, cells were treated where indicated (+) with PK (3.3 μg/mg of protein) at 37 °C for 2 min. The proteins were then trichloroacetic acid-precipitated, separated by SDS-PAGE, and immunoblotted against α-PrP antibody SAF61. For the Triton/DOC insolubility assay, after lysis in Triton/DOC buffer, lysates were ultracentrifuged to separate detergent-soluble (*S*) and insoluble (*P*) molecules. The proteins were trichloroacetic acid-precipitated, and PrPΔGPI was separated by SDS-PAGE and analyzed by Western blotting. *H*, diglycosylated PrP; *M*, monoglycosylated PrP; *U*, unglycosylated PrP; *, immunoglobulin chains.

centrifugation step and trichloroacetic acid-precipitated. PrPs were analyzed by Western blotting.

RESULTS

Expression and Characterization of PrPΔGPI in Transfected FRT Cells—Polarized epithelial FRT (Fischer rat thyroid) cells, previously used to characterize the exocytic pathway of PrP^C (16, 17) and of an inherited pathological PrP mutant (28), were stably transfected with a PrP version lacking the GPI anchor attachment signal (PrPΔGPI) (23). Although PrPΔGPI was previously shown to be predominantly unglycosylated in both cells and animals (23, 24), in our hands it migrated as three major bands corresponding to unglycosylated (*U*), monoglycosylated (*M*), and highly diglycosylated isoforms (*H*), similarly to PrP^C (Fig. 1*A*). This discrepancy could be explained by different conformations of the different isoforms of PrPΔGPI or by particular sugar modifications that could mask the epitopes recognized by some antibodies. Indeed, although all isoforms of PrP^C were equally well immunoprecipitated by the three different antibodies used (α-N-terminal (SAF32, Fig. 1, *lane 1*), α-C-terminal (SAF61, *lane 3*), and α-3F4 tag (PRI308, *lane 2*)), in the case of PrPΔGPI only SAF32 and SAF61 antibodies recognized all glycoforms, whereas PRI308 specifically recognized only the unglycosylated form (Fig. 1*A*). Because the α-3F4 antibody recognizing the same epitope of PRI308 was previously used to characterize PrPΔGPI (23), this could explain why it was previously thought to be unglycosylated (23, 24).

In support of our findings, inhibition of *N*-glycosylation either with PGNaseF digestion or tunicamycin treatment reduced PrPΔGPI to a single band corresponding to the unglycosylated PrP isoform (Fig. 1*B*) similar to the wild-type protein as previously shown (28). To characterize the oligosaccharide chains of PrPΔGPI, we performed a deglycosylation assay using either EndoH or neuraminidase (27) (Fig. 1*B*). Differently from PrP^C, which in the same cells was resistant to EndoH and sensitive to neuraminidase digestion (28), PrPΔGPI was completely resistant to both treatments (Fig. 1*B*). These data suggest that PrPΔGPI displays different oligosaccharide chains compared with PrP^C. Thus, some of the glycan modification enzymes (as well as the sialidases) have no access to the complex *N*-oligosaccharide chains of PrPΔGPI either because of its abnormal folding and/or because of its retention in an intracellular compartment where these enzymes are not present. Furthermore, pulse-chase experiments showed that in addition to the three isoforms present at the steady state (*U*, *M*, and *H*) PrPΔGPI was also synthesized as an immature diglycosylated precursor (*I*) (Fig. 1*C*) that has also been described for PrP^C (16). Interestingly, the level of PrPΔGPI does not decrease even after 6 h of chase (Fig. 1*C*), indicating that the protein is more stable than the wild type, which in FRT cells has a half-life of about 2 h (Fig. 1*C*) (16).

The longer half-life of PrPΔGPI could derive from an altered folding of the protein that would aggregate and then become resistant to degradation. To test this hypothesis we analyzed the scrapie-like characteristics of PrPΔGPI by PK-resistance and Triton-DOC insolubility assays (27) (Fig. 1*D*, *right panel*). By treating 1 mg of total protein in cellular lysates with 3.3 μg of PK for 2 min at 37 °C (16), we found that PrPΔGPI is entirely digested by the enzyme similarly to PrP^C (Fig. 1*D*, *left panel*). Moreover, no sedimentation was found after centrifugation of

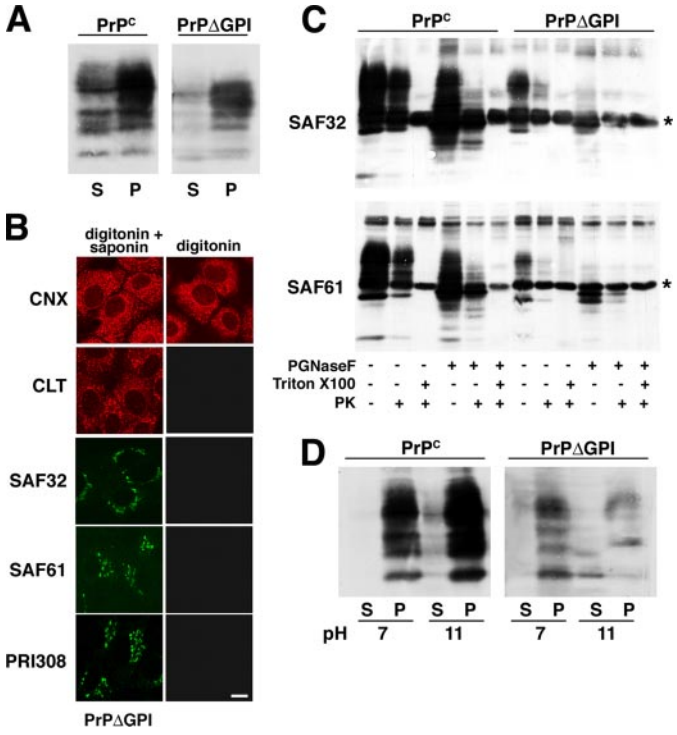

FIGURE 2. **PrPΔGPI is extrinsically linked to cellular membranes and does not acquire a transmembrane topology.** *A*, FRT cells expressing PrP^C and PrPΔGPI were lysed in TX-114 buffer (see "Experimental Procedures") and the aqueous (*S*) and detergent (*P*) phases were analyzed for the presence of PrPs by SDS-PAGE and Western blotting. *B*, FRT cells expressing PrPΔGPI were grown on coverslips and treated with cold digitonin before fixing with 2% paraformaldehyde and eventually permeabilized with 0.075% saponin. The cells were then incubated with either α-PrP mAbs (SAF32, SAF61, and PRI308) or with antibodies against CNX or calreticulin (*CLT*) and then treated with α-mouse and α-rabbit secondary antibody conjugated with fluorescein isothiocyanate or TRITC. *Bar*, 10 μm. The samples were then examined by confocal microscopy by a Zeiss laser scanning confocal microscope (LSCM 510). *C*, PK protection assay. Microsomes were prepared as described under "Experimental Procedures" and either left untreated or incubated with 250 μg/ml PK in the absence or presence of Triton X-100. After immunoprecipitation using either SAF32 or SAF61, the samples were split in two and either left untreated or incubated for 16 h with 5 units/sample PGNaseF. PrPs were detected by Western blotting using either SAF32 and SAF61. *D*, FRT cells expressing PrP^C and PrPΔGPI were homogenized in 0.25 M sucrose at pH 7.5 or 11, and after ultracentrifugation (see "Experimental Procedures") the recovered aqueous (*S*) and detergent (*P*) phases were analyzed for the presence of PrPs by SDS-PAGE and Western blotting. *, immunoglobulin chains.

Triton/DOC lysates at 265,000 × *g* for 40 min (Fig. 1*D*, *right panel*). Taken together, these experiments indicate that despite its long half-life (12 h (not shown)) PrPΔGPI does not display the major biochemical hallmarks of scrapie PrP (*i.e.* misfolding and aggregation).

PrPΔGPI Associates with Cellular Membranes but Does Not Assume a Transmembrane Topology—It is possible that the protein without the GPI anchor assumes a transmembrane topology. To test whether PrPΔGPI associated to membranes, Triton X-114 lysates were incubated at 37 °C and separated into aqueous and detergent phases by centrifugation. PrPΔGPI was recovered almost exclusively in the Triton X-114 detergent phase (Fig. 2*A*), indicating that it was associated to cellular membranes.

Then, to understand whether PrPΔGPI assumes a transmembrane topology, we analyzed the accessibility of specific antibodies to N- or C-terminal PrP epitopes exposed on cytosolic surfaces of intracellular membranes (Fig. 2, *B* and *C*). In a first approach, we used cold digitonin to allow a limited permeabilization of the plasma membrane but not of the intracellular membranes such that only cytosolic epitopes of proteins were accessible (Fig. 2*B*). Under these conditions, as control we could show an ER staining using an CNX antibody against an epitope exposed on the cytosolic side of the endoplasmic reticulum (ER) but not by using an α-calreticulin antibody against an epitope present in the lumen of this organelle (Fig. 2*B*). By using antibodies against the N- or C-terminal PrP sequence or against the 3F4 tag, which spans amino acids 109–112 of human PrP, we did not detect any PrP staining (Fig. 2*B*), suggesting that PrPΔGPI did not span the membranes either with an N- or a C-terminal orientation. The same result was obtained for PrP^C (supplemental Fig. 1).

To exclude that both C- and N-terminal domains were inaccessible in the ER lumen, as is the case of a double-spanning peptide, we analyzed the topology of the PrP mutant by performing a protease protection assay (see "Experimental Procedures") on isolated microsomal vesicles, as previously published (32) (Fig. 2*C*). In this assay, full protection from digestion by exogenous protease indicates complete translocation into the ER lumen, whereas digestion of specific domains generating discrete protease-protected fragments indicates a membrane-spanning topology whose exact orientation can be clarified by identification of the protected fragments with epitope-specific antibodies. We also used PGNaseF to reduce the protein to a single band. After PK treatment, only full-length PrP and no C- or N-terminal PrP fragments could be detected using both C- or N-terminal antibodies (Fig. 2*C*), indicating that PrPΔGPI, similar to PrP^C, was completely translocated into the ER and does not assume a transmembrane topology (33). Note that a high percent of PrP was also digested by PK in absence of detergent. It is expected that a significant population of PrP will be vulnerable to PK digestion also in the absence of detergent because mechanical disruption of cells results in a heterogeneous population of membranes; that is, membrane fragments, "inside-out" vesicles, and vesicles that have maintained their natural polarity. Upon PK digestion, only the fully translocated PrP in the latter vesicles will be protected. The other population of PrP in the former two types of membranes will be vulnerable to digestion by PK.

To confirm that PrPΔGPI was extrinsically associated to membranes, we performed a detergent-free extraction at neutral or basic pH (34) (Fig. 2*D*). In this assay intrinsic membrane proteins such as transmembrane and GPI-anchored proteins cannot be extracted with both pH conditions, whereas extrinsic proteins are extracted only at basic pH. Although PrP^C was recovered in the insoluble phase after both neutral and basic pH extraction, a fraction of PrPΔGPI, in particular the unglycosylated form, was extracted at basic pH (Fig. 2*D*), suggesting that it was extrinsically attached to the membranes.

PrPΔGPI Association with DRMs—Association to rafts might have a role in the conversion process (10, 11, 28, 35–37). Because PrPΔGPI associates to membranes and has been shown to sustain infection, we analyzed whether it associates with DRMs and the characteristics of this association.

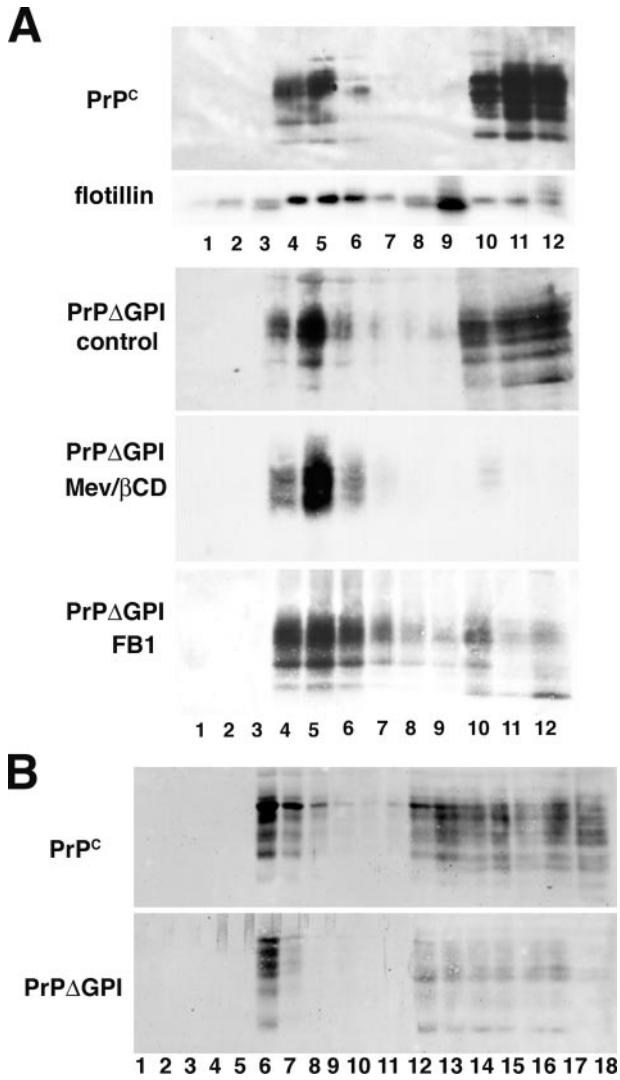

FIGURE 3. **PrPΔGPI associates to DRMs independently from cholesterol and sphingolipids.** *A*, FRT cells expressing PrPΔGPI were grown on 150-mm dishes and treated or not (control) with mevinolin and β-cyclodextrin (*Mev/β-CD*) or fumonisin B1 (*FB1*) as previously described (17). FRT cells expressing PrP^C were used as control. After lysis in 1% Triton X-100, 2 mg of total proteins were run through a two-step (5–30%) sucrose density gradient, as described under "Experimental Procedures." Twelve fractions were collected from the top to bottom of the tube after centrifugation to equilibrium, and PrP and flotillin were revealed by Western blotting. *B*, post-nuclear supernatants from FRT cells expressing either PrP^C or PrPΔGPI were prepared in absence of detergent, and an OptiPrep two-step gradient (0–20%) was performed as described under "Experimental Procedures." Eighteen fractions were collected from the top to bottom of the tube after centrifugation to equilibrium, and PrP was revealed by Western blotting.

DRMs were purified by sucrose density gradients from FRT cells expressing either PrP^C or PrPΔGPI after lysis in cold TX-100 (Fig. 3*A*). The average of four different experiments showed that the same amount (about 50%) both of PrP^C and PrPΔGPI floated to the lighter DRM fractions. We then depleted the cells of cholesterol and sphingolipids, the two major raft components, and analyzed the effect of these treatments on its flotation rate. Surprisingly, we found that DRM association of PrPΔGPI was not perturbed by any of the treatments (Fig. 3*A*), different from what has been shown for PrP^C in the same cells (17). This suggests that the GPI anchor-independent raft association of PrPΔGPI does not depend on cholesterol or sphingolipids.

TABLE 1

Analysis of the lipid species coimmunoprecipitated with PrP^C or PrPΔGPI in the DRM fractions after purification on sucrose density gradients

Nanomoles from each lipid species were determined and expressed in relative percentages. Values represent the mean of three independent experiments ± S.D. SM, sphingomyelin; PC, phosphatidylcholine; PS, phosphatidylserine; PE, phosphatidylethanolamine.

Immunoprecipitates	SM	PC	PS	PE	Cholesterol
PrP^C	9 ± 2	18 ± 2.6	7 ± 1.1	6 ± 1.5	60 ± 5.5
PrPΔGPI	8 ± 1.5	15 ± 1.1	6 ± 1.8	4 ± 1.2	67 ± 5.5

The different effect of either cholesterol and sphingolipid depletion on PrP^C and PrPΔGPI flotation could be due to a different lipid composition of the membrane microdomains to which the two proteins associated. We applied a recent published method (38) to analyze the lipid composition of DRMs associated with PrP^C and PrPΔGPI. However, analysis of the lipids coimmunoprecipitating with PrP^C and PrPΔGPI in the raft fractions of sucrose gradients did not reveal any significant differences in the amount of cholesterol and sphingomyelin associated to PrP^C and PrPΔGPI (Table 1). These results suggest that the two proteins associate with a similar membrane compartment, albeit in different ways.

Because several observations have raised concerns that cell extraction with detergents may generate non-physiological clusters of raft lipids and proteins (31), we isolated rafts from cells fractionated in the absence of detergents (Fig. 3*B*) according to a previously published protocol (31). By using this procedure, both PrPΔGPI and PrP^C could be recovered in the raft fractions (Fig. 3*B*), thus suggesting that this association is not a consequence of detergent addition and confirming that it is not mediated by the GPI anchor.

Analysis of Cellular Distribution of PrPΔGPI—We next analyzed the intracellular localization of PrPΔGPI by indirect immunofluorescence and confocal analysis of FRT cells co-labeled with antibodies directed against PrP and different intracellular compartment markers (Fig. 4*A*). PrPΔGPI colocalized extensively with giantin, a marker of the Golgi apparatus (Fig. 4*A*), whereas no colocalization was found with markers of ER such as CNX and of the endo-lysosomal pathway, such as early endosomal antigen 1 and lysotracker (Fig. 4*A*). This localization pattern was very similar to the one of PrP^C in the same cells (28). However, differently to PrP^C (16, 28), no plasma membrane (PM) signal of PrPΔGPI was found (Fig. 4*A*). To rule out the possibility that the immunofluorescence signal at the PM was below detection levels, we analyzed the surface localization of PrPΔGPI by a biotinylation assay (Fig. 4*B*) and by confocal microscopy (not shown) in cells grown on filters in polarized conditions where the exocytic transport to the surface is enhanced compared with cells grown on coverslips (17, 28). Both of these experiments confirmed that PrPΔGPI is not present on the cell surface of FRT cells (Fig. 4*B*).

Analysis of Secretion of PrPΔGPI—The data presented above suggested that PrPΔGPI was secreted. To verify this hypothesis, media from PrP^C- and PrPΔGPI-expressing FRT cells were collected after overnight culture and analyzed for the presence of

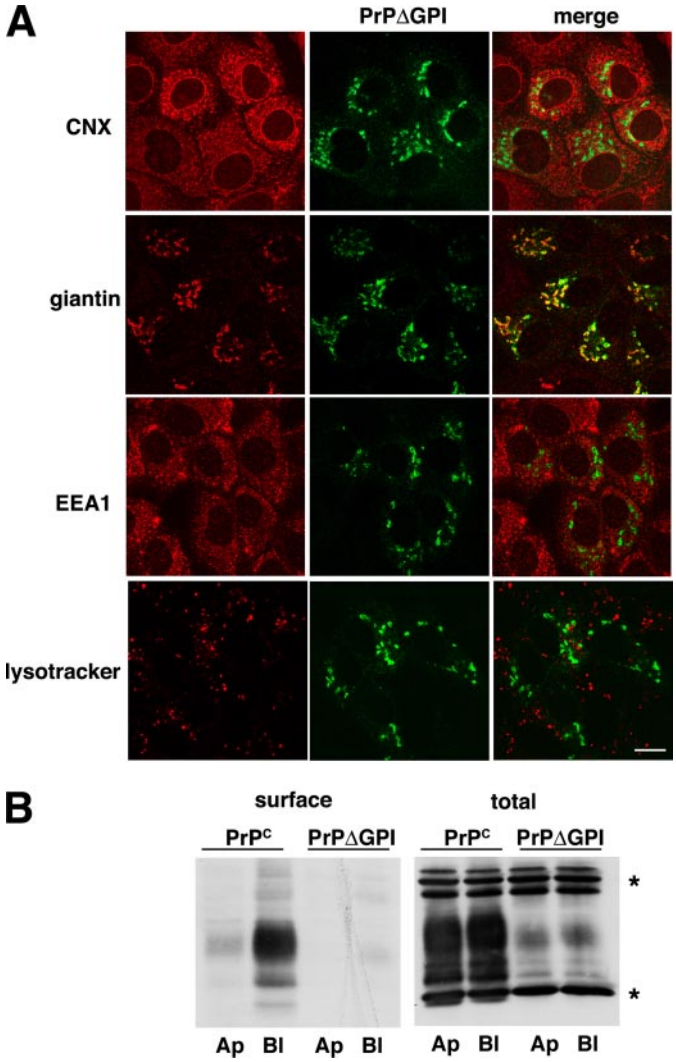

FIGURE 4. **PrPΔGPI localizes mainly in the Golgi apparatus and is absent from the plasma membrane.** *A*, FRT cells expressing PrPΔGPI were grown on coverslips and fixed with 2% paraformaldehyde and permeabilized with 0.075% saponin. They were then incubated with the α-PrP mAb (SAF32) and with primary polyclonal antibodies against different markers of intracellular compartments, *e.g.* CNX, giantin, and early endosomal antigen 1 (*EEA1*) and then treated with α-mouse and α-rabbit secondary antibody conjugated with fluorescein isothiocyanate or TRITC. Lysotracker was used to label lysosomes for 1 h *in vivo* before fixation and confocal imaging. *Bar*, 10 μm. The samples were then examined in a Zeiss laser scanning confocal microscope (LSCM 510). *B*, FRT cells were grown on filters for 5 days. Surface-expressed PrP^C and PrPΔGPI were selectively biotinylated from the apical (*Ap*) or basolateral (*BL*) side. The cell lysates were collected and immunoprecipitated with SAF32 antibody, and PrPs were revealed by Western blotting using both horseradish peroxidase-conjugated streptavidin (*left panel*) or SAF61 antibody (*right panel*). *, immunoglobulin chains.

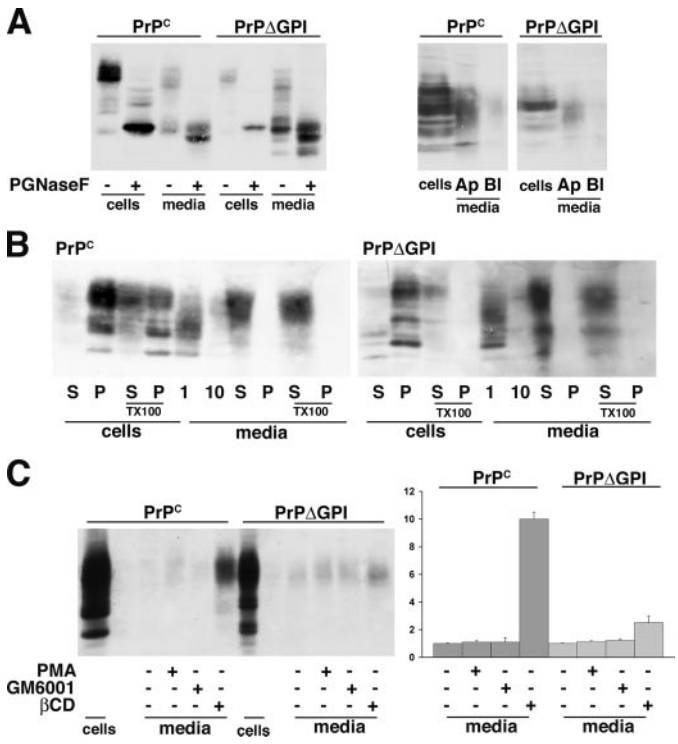

FIGURE 5. **PrPΔGPI is secreted in a soluble form in a metalloprotease-independent and βCD-dependent polarized manner.** Cell lysates and overnight media from PrP^C- and PrPΔGPI-expressing FRT cells were (*A*) immunoprecipitated with SAF32 antibody, digested (+) or not (−) for 16 h with 5units/sample of PGNaseF and analyzed by Western blots (*left panel*). Alternatively, FRT cells were grown on Transwell filters for 5 days to collect overnight apical and basolateral media (*right panel*). Note that in contrast to the *left panel*, the lanes of lysates and media in the *right panels* are not quantitatively representative since the ratio cells/media is 1:3 in the case of PrP^C and 3:1 in the case of PrPΔGPI. *Ap*, apical; *BL*, basolateral. *B*, after submitting overnight cell culture media to sequential centrifugation steps with increasing centrifugal forces (*1*, 1,000 × *g*; *10*, 10,000 × *g*) as described under "Experimental Procedures" (40), ultracentrifugation at 100,000 × *g* was performed to separate soluble (*S*) and membrane-associated (*P*) proteins. Ultracentrifuged cell homogenates were used as controls. Triton X-100 was used to release membrane-associated proteins in the soluble fraction. All samples were then trichloroacetic acid-precipitated and analyzed by Western blotting using SAF32 antibody. *C*, immunoprecipitation with SAF32 antibody, and Western blotting analysis was performed on cell culture media from PrP^C- and PrPΔGPI-expressing FRT cells collected after 7 h of treatment with either the zinc metalloprotease hydroxamate-based inhibitor GM6001, phorbol 12-myristate 13-acetate (*PMA*), or βCD. Quantization of three independent experiments is shown in the graphs. *Error bars* are shown.

the proteins by Western blots. Interestingly, although we found only a 1–5% of the total PrP^C in the cell media (Fig. 5*A*, *left panel*, compare the *first* and *third lanes*), more than 90% of PrPΔGPI was secreted (Fig. 5*A*, compare and *fifth* and *seventh lanes*). To understand whether the secreted polypeptide corresponded to the full-length protein or to a proteolytic product, we treated the lysates with PGNaseF. We found that both the full-length protein and lower molecular weight products were secreted both for PrP^C and PrPΔGPI (Fig. 5*A*, *fourth* and *eighth lanes*). The lower bands could represent the shed PrP forms, recently described (39). Interestingly, by collecting separately the apical and basolateral media of FRT cells grown on Transwell filters, we found that both PrP^C and PrPΔGPI were selectively secreted from the apical domain of the plasma membrane (Fig. 5*A*, *right panels*) despite the prevalent basolateral localization of PrP^C in FRT cells (16).

To investigate whether the fraction of PrP found in the cell media was released in association with membranes rather than as a soluble product, overnight cell culture medium was submitted to sequential centrifugation steps with increasing centrifugal forces as described above (40). Neither PrP^C nor PrPΔGPI in the media formed a pellet at 100,000 × *g*, indicating that the majority of the protein was released as soluble product and was not membrane-associated (Fig. 5*B*).

Because it has been shown that PrP^C is constitutively shed either by a mechanism involving a secretase-like proteolytic cleavage of the protein or a phospholipase cleavage of the GPI

anchor moiety (39), we investigated the mechanism implicated in the secretion of PrPΔGPI. To discriminate between protease-dependent and -independent secretion, PrP immunoprecipitation and Western blot analysis were performed on media from cells grown for 7 h in the presence of 1) the zinc metalloprotease hydroxamate-based inhibitor GM6001, 2) the phorbol 12-myristate 13-acetate, an activator of metalloprotease-mediated APP and PrP^C shedding (39), or 3) βCD, which has been shown to stimulate a metalloprotease-independent cell release of PrP^C (39) (Fig. 5*C*). Interestingly, in our cell system PrP^C and PrPΔGPI secretion was not affected by treatment with GM6001 and phorbol 12-myristate 13-acetate but was increased by βCD. Statistical analysis showed that PrP^C and PrPΔGPI secretion were increased 10- and 2-fold, respectively, after βCD treatment (Fig. 5*C*), suggesting that most of the protein was released by a metalloprotease-independent mechanism. It has been suggested that the βCD-dependent shedding of PrP^C is linked to cleavage of the GPI anchor by the action of a phospholipase (39). Because this is not possible for a protein that is not GPI-anchored, the βCD-dependent PrP secretion is likely due to the extraction of the protein (with or without GPI anchor) from cell membranes. However, we cannot exclude that PrPΔGPI interacts with another GPI-anchored protein that would be released into the media upon βCD treatment.

DISCUSSION

Several lines of evidence suggest that prion replication is a posttranslational event involving many factors. However, the intracellular site and the mechanisms leading to prion replication and their cell toxicity are not yet understood. Kinetic studies of PrP mutants synthesized in Chinese hamster ovary cells suggest that individual steps in the formation of PrP^{Sc} may take place in at least three different cellular locations: the ER, the cell surface, and the endo-lysosomal compartment (3, 41). Interestingly, it has been recently shown that an anchorless version of PrP, although able to sustain scrapie replication, does not generate any characteristic symptoms of the disease in scrapie-infected transgenic mice, thus implying a role of the GPI anchor in the pathogenesis of prion diseases. One possibility to explain these findings is that the lack of the GPI anchor determines defects in the trafficking and localization of the anchorless protein, which might in turn affect the pathogenesis of these disorders. To provide the field a better understanding of the biosynthesis and cell biology of the anchorless PrP, which thereby may lead toward a better understanding of the cellular site of prion pathogenesis, we have studied the metabolism and the intracellular trafficking of an anchorless version of PrP, PrPΔGPI, in transfected FRT cells that we have previously used to study PrP^C (16, 17, 28).

At steady state, PrPΔGPI was expressed at lower levels than PrP^C (Fig. 1, *A* and *B*), as previously shown in other cell systems and animals (23, 24). In contrast with previous findings (23, 24) we also demonstrated that PrPΔGPI was highly glycosylated and was detected in Western blots as three major bands corresponding to the different glycoforms (*U*, *M*, and *H*) of the prion protein (Fig. 1*A*), suggesting that previous published results were probably due to the use of antibodies not recognizing the glycosylated forms of PrPΔGPI (23, 24). We also found that PrPΔGPI displays different oligosaccharide chains compared with PrP^C (Fig. 1*B*), thus indicating that some glycan modification enzymes (as well as the sialidases) have no access to the complex *N*-oligosaccharide chains of PrPΔGPI either because of its abnormal folding and/or because of its retention in an intracellular compartment where these enzymes are not present. This result also indicates that proper PrP glycosylation is contingent upon the C terminus (and possibly the GPI anchor) and points to a functional relationship between the maturation and the trafficking of prions. In addition, PrPΔGPI has a longer half-life than PrP^C (Fig. 1*C*), but this event is not related to the acquisition of any of the scrapie-like properties (Fig. 1*D*). Interestingly, in scrapie-infected transgenic mice expressing the anchorless version of PrP, a marked change in the quality of the PrP^{Sc} found in the brain has been demonstrated (24). Indeed, instead of the usual diffuse and punctate nonamyloid pattern deriving from the conformational conversion of PrP^C, in the case of PrPΔGPI conversion a thioflavin S-positive PrP^{Sc} amyloid pattern was observed (24). Among the several hypotheses to explain this event, the authors suggest that amyloid formation could be favored because this PrP mutant largely lacks carbohydrates. However, because we show here that the protein is correctly glycosylated we postulated that the formation of the biggest aggregates could be promoted either by the long half-life of PrPΔGPI (that would have more time to be converted and to accumulate) or due to a different intracellular localization of the anchorless protein. To support this latter hypothesis we analyzed the intracellular pathway of this form.

By confocal microscopy, we found that PrPΔGPI extensively colocalizes with giantin, a marker of the Golgi apparatus (Fig. 4*A*), whereas it was not found at the plasma membrane (Fig. 4*B*). The lack of PM localization of PrPΔGPI could explain why the symptoms of the disease in Tg mice for anchorless PrP were much milder. Indeed, it is conceivable that the PM represents the place from where prions induce toxicity. This hypothesis is consistent with the growing body of evidence that PrP^C could function as a signaling molecule, as do many GPI-anchored proteins (42), shown by the fact that antibody cross-linking of PrP^C on the cell surface of hippocampal neurons induces cell death (43). This is also supported by the recent finding that the expression of a PrP variant lacking 40 central residues (94–134) induces a rapidly progressive, lethal phenotype with extensive central and peripheral myelin degeneration in mice, suggesting that PrP^C has a neurotrophic effect (44). Thus, the lack of GPI anchor of PrPΔGPI and the consequent lack of PM localization from where PrP^C probably performs its normal function and from where PrP^{Sc} gains a pathological dysfunction could explain why PrPΔGPI does not induce clinical symptoms in scrapie-infected transgenic mice even though it is convertible into the scrapie form (24). This hypothesis is also consistent with the finding that transgenic mice heterozygous for both wild-type and anchorless PrP died faster than wild-type mice (24). It is possible that in these mice, anchorless PrP accelerates scrapie disease because it promotes the spreading of prion infection by its secretion.

Despite the absence of the lipid anchor PrPΔGPI was recovered almost exclusively in the Triton X-114 detergent phase after aqueous-detergent phase separation (Fig. 2*A*), although it

did not assume a transmembrane topology and was extracted at basic pH (Fig. 2*D*). These results indicated that it was extrinsically attached to the cellular membranes. We also found that PrPΔGPI floats to the lighter DRM fractions of sucrose density gradients in a cholesterol- and sphingolipid-independent manner (Fig. 3). These findings support previous data that raft-association of PrP is independent of the GPI anchor (25) and is in contrast with recent data showing that in brain extracts from anchorless PrP-expressing mice, it did not float to DRM fractions (24). These contrasting data could be explained by the different methods and conditions used for the flotation assay and might indicate that in more complex systems other factors could participate in PrP raft association, thus modifying its flotation profile. In addition, our data might indicate that the nature of the raft environment to which the wild-type or the anchorless protein associate are different, which could affect the behavior of the two proteins. Alternatively, if the raft environment is the same, as our preliminary analysis supports (Table 1), it would be the different manner of association to these membranes that would determine differences in behavior.

Interestingly, although the protein is membrane-associated, greater than 90% of PrPΔGPI was recovered in the cell media (Fig. 5*A*), thus explaining the low cellular levels despite its very long half-life. Although secretion of this form was reported before (24), it was never further studied.

It has been shown that PrP^C can be released into the medium of human neuroblastoma SH-SY5Y cells by either a protease- or phospholipase-dependent shedding (39). Interestingly, in our cell system PrP^C and PrPΔGPI secretion was stimulated by βCD. However, although secretion of PrP^C was increased 10-fold by βCD, it was increased only 2-fold for PrPΔGPI. This difference is probably due to the different manner of association to the cellular membranes of these two PrP variants. Indeed, it has been suggested that the βCD-dependent shedding of PrP^C was linked to the cleavage of the GPI anchor by the action of a phospholipase (39). Because this is not an option in the case of anchorless PrP, we alternatively propose that the βCD-dependent PrP secretion is due to the extraction of the protein (with or without GPI anchor) from cell membranes after raft perturbation. However, we cannot exclude that PrPΔGPI interacts with another GPI-anchored protein, which would be released by the action of a phospholipase upon βCD treatment.

We also discovered that PrP secretion is a polarized event because both PrP^C and PrPΔGPI were secreted from the apical domain of the plasma membrane (Fig. 5*A*, *right panels*) despite the prevalent basolateral localization of PrP^C in FRT cells (16). This is quite interesting and could be in relation with the fact that in polarized cells infection seems to be a polarized event (45). Moreover, this behavior could be very important for the transfer of infectivity from one cell to another. Indeed, it has been recently shown that infected Rov cells release PrP^C and PrP^{Sc} in association with exosomes, membranous vesicles that are secreted upon fusion of multivesicular endosomes with the plasma membrane (46). However, despite these findings, our results indicate that both PrP^C and PrPΔGPI released in the media are not associated to membrane vesicles but are released in a soluble form (Fig. 5*B*).

Finally, our findings, *e.g.* the altered localization of the PrPΔGPI as substrate for the conversion reaction, the lack of PM localization, and its secretion in the extracellular space, might explain the lack of development of the disease in infected Tg mice expressing anchorless PrP. If this is the case, it is possible that the PM localization of the substrate (PrP^C) and of its misfolded form (PrP^{Sc}) are necessary to stimulate the prion misfunction that leads to symptomatic disease.

Acknowledgments—We thank Dr. Sylvain Lehmann for the kind gift of the PrPΔGPI cDNA. We also thank Dr. Jacques Grassi for the generous gift of several α-PrP antibodies and Dr. Chris Bowler and Duncan Browman for critical reading of the manuscript.

REFERENCES

1. Prusiner, S. B. (1998) *Proc. Natl. Acad. Sci. U. S. A.* **95,** 13363–13383
2. Horwich, A. L., and Weissman, J. S. (1997) *Cell* **89,** 499–510
3. Campana, V., Sarnataro, D., and Zurzolo, C. (2005) *Trends Cell Biol.* **15,** 102–111
4. Caughey, B., and Raymond, G. J. (1991) *J. Biol. Chem.* **266,** 18217–18223
5. Borchelt, D. R., Taraboulos, A., and Prusiner, S. B. (1992) *J. Biol. Chem.* **267,** 16188–16199
6. Taraboulos, A., Raeber, A. J., Borchelt, D. R., Serban, D., and Prusiner, S. B. (1992) *Mol. Biol. Cell* **3,** 851–863
7. Lee, K. S., Magalhaes, A. C., Zanata, S. M., Brentani, R. R., Martins, V. R., and Prado, M. A. (2001) *J. Neurochem.* **79,** 79–87
8. Marella, M., Lehmann, S., Grassi, J., and Chabry, J. (2002) *J. Biol. Chem.* **277,** 25457–25464
9. Naslavsky, N., Stein, R., Yanai, A., Friedlander, G., and Taraboulos, A. (1997) *J. Biol. Chem.* **272,** 6324–6331
10. Naslavsky, N., Shmeeda, H., Friedlander, G., Yanai, A., Futerman, A. H., Barenholz, Y., and Taraboulos, A. (1999) *J. Biol. Chem.* **274,** 20763–20771
11. Taraboulos, A., Scott, M., Semenov, A., Avrahami, D., Laszlo, L., Prusiner, S. B., and Avraham, D. (1995) *J. Cell Biol.* **129,** 121–132
12. Zurzolo, C., van Meer, G., and Mayor, S. (2003) *EMBO Rep.* **4,** 1117–1121
13. Simons, K., and Toomre, D. (2000) *Nat. Rev. Mol. Cell. Biol.* **1,** 31–39
14. Simons, K., and Ikonen, E. (1997) *Nature* **387,** 569–572
15. Brown, D. A., and London, E. (1998) *Annu. Rev. Cell Dev. Biol.* **14,** 111–136
16. Sarnataro, D., Paladino, S., Campana, V., Grassi, J., Nitsch, L., and Zurzolo, C. (2002) *Traffic* **3,** 810–821
17. Sarnataro, D., Campana, V., Paladino, S., Stornaiuolo, M., Nitsch, L., and Zurzolo, C. (2004) *Mol. Biol. Cell* **15,** 4031–4042
18. Vey, M., Pilkuhn, S., Wille, H., Nixon, R., DeArmond, S. J., Smart, E. J., Anderson, R. G., Taraboulos, A., and Prusiner, S. B. (1996) *Proc. Natl. Acad. Sci. U. S. A.* **93,** 14945–14949
19. Madore, N., Smith, K. L., Graham, C. H., Jen, A., Brady, K., Hall, S., and Morris, R. (1999) *EMBO J.* **18,** 6917–6926
20. Kaneko, K., Vey, M., Scott, M., Pilkuhn, S., Cohen, F. E., and Prusiner, S. B. (1997) *Proc. Natl. Acad. Sci. U. S. A.* **94,** 2333–2338
21. Kocisko, D. A., Come, J. H., Priola, S. A., Chesebro, B., Raymond, G. J., Lansbury, P. T., and Caughey, B. (1994) *Nature* **370,** 471–474
22. Lawson, V. A., Priola, S. A., Wehrly, K., and Chesebro, B. (2001) *J. Biol. Chem.* **276,** 35265–35271
23. Rogers, M., Yehiely, F., Scott, M., and Prusiner, S. B. (1993) *Proc. Natl. Acad. Sci. U. S. A.* **90,** 3182–3186
24. Chesebro, B., Trifilo, M., Race, R., Meade-White, K., Teng, C., LaCasse, R., Raymond, L., Favara, C., Baron, G., Priola, S., Caughey, B., Masliah, E., and Oldstone, M. (2005) *Science* **308,** 1435–1439
25. Walmsley, A. R., Zeng, F., and Hooper, N. M. (2003) *J. Biol. Chem.* **278,** 37241–37248
26. Zurzolo, C., Lisanti, M. P., Caras, I. W., Nitsch, L., and Rodriguez-Boulan, E. (1993) *J. Cell Biol.* **121,** 1031–1039

27. Lehmann, S., and Harris, D. A. (1997) *J. Biol. Chem.* **272,** 21479–21487
28. Campana, V., Sarnataro, D., Fasano, C., Casanova, P., Paladino, S., and Zurzolo, C. (2006) *J. Cell Sci.* **119,** 433–442
29. Drisaldi, B., Stewart, R. S., Adles, C., Stewart, L. R., Quaglio, E., Biasini, E., Fioriti, L., Chiesa, R., and Harris, D. A. (2003) *J. Biol. Chem.* **278,** 21732–21743
30. Prinetti, A., Chigorno, V., Tettamanti, G., and Sonnino, S. (2000) *J. Biol. Chem.* **275,** 11658–11665
31. Macdonald, J. L., and Pike, L. J. (2005) *J. Lipid Res.* **46,** 1061–1067
32. Hegde, R. S., Mastrianni, J. A., Scott, M. R., DeFea, K. A., Tremblay, P., Torchia, M., DeArmond, S. J., Prusiner, S. B., and Lingappa, V. R. (1998) *Science* **279,** 827–834
33. Stewart, R. S., and Harris, D. A. (2003) *J. Biol. Chem.* **278,** 45960–45968
34. Brown, D. A., and Rose, J. K. (1992) *Cell* **68,** 533–544
35. Baron, G. S., Wehrly, K., Dorward, D. W., Chesebro, B., and Caughey, B. (2002) *EMBO J.* **21,** 1031–1040
36. Sanghera, N., and Pinheiro, T. J. (2002) *J. Mol. Biol.* **315,** 1241–1256
37. Kazlauskaite, J., and Pinheiro, T. J. (2005) *Biochem. Soc. Symp.* **72,** 211–222
38. Tivodar, S., Paladino, S., Pillich, R., Prinetti, A., Chigorno, V., van Meer, G., Sonnino, S., and Zurzolo, C. (2006) *FEBS Lett.* **580,** 5705–5712
39. Parkin, E. T., Watt, N. T., Turner, A. J., and Hooper, N. M. (2004) *J. Biol. Chem.* **279,** 11170–11178
40. Raposo, G., Nijman, H. W., Stoorvogel, W., Liejendekker, R., Harding, C. V., Melief, C. J., and Geuze, H. J. (1996) *J. Exp. Med.* **183,** 1161–1172
41. Harris, D. A. (2003) *Br. Med. Bull.* **66,** 71–85
42. Mayor, S., and Riezman, H. (2004) *Nat. Rev. Mol. Cell Biol.* **5,** 110–120
43. Solforosi, L., Criado, J. R., McGavern, D. B., Wirz, S., Sanchez-Alavez, M., Sugama, S., DeGiorgio, L. A., Volpe, B. T., Wiseman, E., Abalos, G., Masliah, E., Gilden, D., Oldstone, M. B., Conti, B., and Williamson, R. A. (2004) *Science* **303,** 1514–1516
44. Baumann, F., Tolnay, M., Brabeck, C., Pahnke, J., Kloz, U., Niemann, H. H., Heikenwalder, M., Rulicke, T., Burkle, A., and Aguzzi, A. (2007) *EMBO J.* **26,** 538–547
45. Paquet, S., Sabuncu, E., Delaunay, J. L., Laude, H., and Vilette, D. (2004) *J. Virol.* **78,** 7148–7152
46. Fevrier, B., Vilette, D., Archer, F., Loew, D., Faigle, W., Vidal, M., Laude, H., and Raposo, G. (2004) *Proc. Natl. Acad. Sci. U. S. A.* **101,** 9683–9688

Characterization of the Properties and Trafficking of an Anchorless Form of the Prion Protein

Vincenza Campana, Anna Caputo, Daniela Sarnataro, Simona Paladino, Simona Tivodar and Chiara Zurzolo

J. Biol. Chem. 2007, 282:22747-22756.
doi: 10.1074/jbc.M701468200 originally published online June 7, 2007
